



HAL
open science

Discontinuous-Skeletal methods with linear and quadratic reconstructions for the elliptic obstacle problem

Matteo Cicuttin, Alexandre Ern, Thirupathi Gudi

► **To cite this version:**

Matteo Cicuttin, Alexandre Ern, Thirupathi Gudi. Discontinuous-Skeletal methods with linear and quadratic reconstructions for the elliptic obstacle problem. 2018. hal-01718883v1

HAL Id: hal-01718883

<https://hal.science/hal-01718883v1>

Preprint submitted on 27 Feb 2018 (v1), last revised 3 May 2019 (v2)

HAL is a multi-disciplinary open access archive for the deposit and dissemination of scientific research documents, whether they are published or not. The documents may come from teaching and research institutions in France or abroad, or from public or private research centers.

L'archive ouverte pluridisciplinaire **HAL**, est destinée au dépôt et à la diffusion de documents scientifiques de niveau recherche, publiés ou non, émanant des établissements d'enseignement et de recherche français ou étrangers, des laboratoires publics ou privés.

Discontinuous-Skeletal methods with linear and quadratic reconstructions for the elliptic obstacle problem*

Matteo Cicuttin[†]

Alexandre Ern[†]

Thirupathi Gudi[‡]

February 27, 2018

Abstract

Discontinuous-skeletal methods are introduced and analyzed for the elliptic obstacle problem in two and three space dimensions. The methods are formulated in terms of face unknowns which are polynomials of degree $k = 0$ or $k = 1$ and in terms of cell unknowns which are polynomials of degree $l = 0$. The discrete obstacle constraints are enforced on the cell unknowns. A priori error estimates of optimal order (up to the regularity of the exact solution) are shown. Specifically, for $k = 0$, the method employs a local linear reconstruction operator and achieves an energy-error estimate of order h , where h is the mesh-size, whereas for $k = 1$, the method employs a local quadratic reconstruction operator and achieves an energy-error estimate of order $h^{\frac{3}{2}-\epsilon}$, $\epsilon > 0$. Numerical experiments in two and three space dimensions illustrate the theoretical results.

Keywords. discontinuous-skeletal method, hybrid high-order method, obstacle problem, error estimates, variational inequalities

Mathematics Subject Classification. 65N15, 65N30, 65N12

1 Introduction

Hybrid Higher Order (HHO) methods have been introduced recently for linear elasticity in [23] and for linear diffusion problems in [25]. HHO methods have been extended to other linear PDEs, such as advection-diffusion [26] and Stokes [27], and to nonlinear PDEs, such as Leray–Lions operators [21], steady incompressible Navier–Stokes equations [24], nonlinear elasticity with infinitesimal deformations [7], and hyperelasticity with finite deformations [1]. HHO methods are formulated in terms of face unknowns which are polynomials of arbitrary order $k \geq 0$ on each mesh face and in terms of cell unknowns which are polynomials of order $l \geq 0$, with $l \in \{k, k \pm 1\}$, in each mesh cell. The cell unknowns can be eliminated locally by static condensation leading to a global transmission problem posed solely in terms of the face unknowns. For this reason, HHO methods are also termed Discontinuous-Skeletal methods. This is the terminology we adopt in this work where we are going to focus on the choice $k \in \{0, 1\}$ for the polynomial degree of the face unknowns and $l = 0$ for the polynomial degree of the cell unknowns. HHO methods offer various assets: they support polyhedral meshes, lead to local conservation principles, and their construction is independent of the space dimension. Lowest-order HHO methods are closely related to the Hybrid Finite Volume method [30], the Compatible Discrete Operator framework [6], and the Mimetic Finite Difference methods [40, 12, 13], see also the unifying viewpoint in [28]. HHO methods have been bridged in [20] to hybridizable discontinuous Galerkin methods [19] and to nonconforming Virtual Element methods [3].

In this work, we devise and analyze a Discontinuous-Skeletal method to approximate the solution of the elliptic obstacle problem in two and three space dimensions. We consider the polynomial degrees $k \in \{0, 1\}$ for the face unknowns and the polynomial degree $l = 0$ for the cell unknowns, and the obstacle constraint is enforced on the cell unknowns. As is customary with Discontinuous-Skeletal methods, their formulation

¹This work was carried over while the third author visited INRIA through the Invited Professorship program.

²Université Paris-Est, CERMICS (ENPC), 77455 Marne-la-Vallée cedex 2, France and INRIA Paris, 75589 Paris, France. email: alexandre.ern@enpc.fr, matteo.cicuttin@enpc.fr

³Department of Mathematics, Indian Institute of Science, Bangalore, India 560012. email: gudi@iisc.ac.in

relies on a local reconstruction operator and a local stabilization operator. The local reconstruction operator produces linear polynomials in each mesh cell for $k = 0$ and quadratic polynomials in each mesh cell for $k = 1$. The local stabilization operator weakly enforces a matching between the face unknowns and the trace of the cell unknowns. Our main result is Theorem 4.1 below where we establish, under reasonable smoothness assumptions on the exact solution, an energy-error estimate of order h^r , where h is the mesh-size, $r = 1$ if $k = 0$ and $r = \frac{3}{2} - \epsilon$, $\epsilon > 0$, if $k = 1$.

Let us put our work in perspective with the literature. The elliptic obstacle problem relies on firm mathematical foundations and appears in many engineering applications; see, among others, the textbooks [33, 35, 39, 43]. The numerical analysis of the two-dimensional elliptic obstacle problem using finite elements was initiated in 1970's in [32, 11]. In [32], a linear finite element method was proposed and analyzed with discrete obstacle constraints enforced at the vertices of the triangulation, whereas in [11], a quadratic finite element method was proposed and analyzed with discrete obstacle constraints enforced at the edge midpoints of the triangulation. The assumption in [11] on the finiteness of the free boundary length was relaxed in [47]. More recently in [46], linear and quadratic discontinuous Galerkin (DG) methods were proposed and analyzed for the elliptic obstacle problem and a frictional contact problem. These methods are designed by enforcing the discrete obstacle constraints at the vertices and the edge midpoints of the triangulation, similarly to the case of conforming linear and quadratic finite elements, respectively. The classical Crouzeix–Raviart nonconforming method was first studied in [48] with the regularity assumption on the exact solution that $u \in W^{s,p}(\Omega)$ with $s < 2 + 1/p$ and $1 < p < \infty$. A refined analysis for the nonconforming method with minimal regularity assumptions is presented in [16] by constructing a novel conforming companion to the nonconforming discrete solution. Mimetic finite difference methods which support general polyhedral meshes were studied in [2]. Mixed and stabilized mixed methods, where both the solution and the Lagrange multiplier are approximated, were analyzed in [36]. Let us emphasize that the analysis in the above articles for the obstacle problem is restricted to two-dimensional problems. The design and analysis of linear conforming finite element methods in three dimensions can be performed similarly to the two-dimensional case. However, the design of a three-dimensional quadratic finite element method that achieves optimal convergence rates (up to the regularity of the exact solution) is not similar to the two-dimensional case. Recently, in [34], a quadratic finite element method enriched with element-wise bubbles was proposed and analyzed for the three-dimensional elliptic obstacle problem. The above literature review shows that a gap still remains concerning the quadratic approximation of the three-dimensional elliptic obstacle problem. The main purpose of the present work is to fill this gap. Let us also emphasize that, from a computational viewpoint, the proposed Discontinuous-Skeletal method is particularly attractive since the discrete obstacle constraints are enforced on the cell unknowns which are constant in each mesh cell. Hence, well-established solvers like active-set methods [37] can be readily used. More broadly, we can mention other works related to the numerical analysis of variational inequalities in computational mechanics, such as boundary contact problems of Signorini type [4, 5, 15, 17, 29, 38, 44, 49, 50] and C^0 interior penalty methods for displacement obstacle clamped plate problems [8, 9].

This article is organized as follows. In Section 2, we present the model problem. In Section 3, we introduce the Discontinuous-Skeletal discretization; we also derive the discrete elliptic obstacle problem and establish its well-posedness. In Section 4, we prove our main result, namely an energy-error estimate of order h for $k = 0$ and of order $h^{\frac{3}{2} - \epsilon}$, $\epsilon > 0$, for $k = 1$. Finally, in Section 5, we present numerical results on two- and three-dimensional test cases to illustrate our error estimate.

2 Model problem

Let $D \subset \mathbb{R}^d$ with $d \in \{2, 3\}$ be an open subset with sufficiently smooth boundary ∂D . Let $H^m(D)$ denote the standard L^2 -based Sobolev space of order $m \geq 0$, and let $\gamma : H^1(D) \rightarrow H^{\frac{1}{2}}(\partial D)$ denote the well-known surjective trace map. More generally, for any subset $G \subseteq D$ (which is typically D or its boundary, a mesh cell or its boundary, or a mesh face), we denote the norm and semi-norm on the standard Sobolev space $W^{s,p}(G)$ by $\|\cdot\|_{W^{s,p}(G)}$ and $|\cdot|_{W^{s,p}(G)}$, where $s \geq 0$ is the order of the derivative and $1 \leq p \leq \infty$ is the exponent in the integration (with the appropriate Lebesgue measure depending on the dimension of G). For simplicity, we denote $\|\cdot\|_{L^2(G)}$ by $\|\cdot\|_G$ and the $L^2(G)$ -inner product by $(\cdot, \cdot)_G$; the same notation is used for vector-valued functions.

We consider the elliptic obstacle problem posed in D with a non-homogeneous Dirichlet condition on ∂D . The data are the load function $f \in L^2(D)$, the Dirichlet value $g \in H^{\frac{1}{2}}(\partial D)$, and the obstacle function

$\chi \in H^1(D) \cap C^0(\bar{D})$ such that $\chi \leq g$ a.e. on ∂D . Define the set

$$\mathcal{K} := \{v \in H^1(D) \mid v \geq \chi \text{ a.e. in } D \text{ and } \gamma(v) = g\}. \quad (2.1)$$

Define the bilinear form $a : H^1(D) \times H^1(D) \rightarrow \mathbb{R}$ and the linear form $\ell : H^1(D) \rightarrow \mathbb{R}$, respectively, by

$$a(w, v) = (\nabla w, \nabla v)_D \quad \text{and} \quad \ell(v) = (f, v)_D. \quad (2.2)$$

The model problem consists of finding $u \in \mathcal{K}$ such that

$$a(u, v - u) \geq \ell(v - u) \quad \forall v \in \mathcal{K}, \quad (2.3)$$

or, equivalently, of minimizing the functional $J(v) := \frac{1}{2}a(v, v) - \ell(v)$ over \mathcal{K} . Owing to the following Browder–Stampacchia Lemma (see [14, 39]), we infer that the model problem (2.3) is well-posed.

Lemma 2.1 (Browder–Stampacchia). *Let H be a real Hilbert space with norm $\|\cdot\|_H$ and let H' denote the dual space of H . Let a be a bilinear form on $H \times H$ satisfying*

$$a(v, v) \geq \alpha \|v\|_H^2 \quad \text{and} \quad |a(w, v)| \leq \xi \|w\|_H \|v\|_H \quad \text{for all } w, v \in H, \quad (2.4)$$

for some positive constants α and ξ . Let \mathcal{K} be a nonempty, closed, convex subset of H and let $\ell \in H'$. Then there exists a unique $u \in \mathcal{K}$ such that $a(u, v - u) \geq \ell(v - u)$ for all $v \in \mathcal{K}$.

In what follows, we make some (reasonable) additional smoothness assumptions on the exact solution. Specifically, we assume that for all $1 < p < \infty$ and all $s < 2 + \frac{1}{p}$, $u \in W^{s,p}(D)$, and that the following complementarity conditions hold true with $\lambda := -\Delta u - f$,

$$\lambda \geq 0 \text{ a.e. in } D, \quad (2.5a)$$

$$\lambda = 0 \text{ in the interior of the set } \{x \in D : u(x) > \chi(x)\}, \quad (2.5b)$$

$$(u - \chi, \lambda)_D = 0. \quad (2.5c)$$

The above assumptions are reasonable once invoking the elliptic regularity theory for obstacle problems if the problem data satisfies additional smoothness assumptions. In particular, if $\chi \in H^2(D)$ and g is the trace of a $H^2(D)$ function, then $u \in H^2(D)$ and the above complementarity conditions hold true [39]. Moreover, if $f \in L^\infty(D) \cap BV(D)$, $g, \chi \in C^3(\bar{D})$ with $g \geq \chi$ on ∂D , and if the boundary ∂D is sufficiently smooth, then $u \in W^{s,p}(D)$ as stated above [10, 11, 39, 47]. In the present work, we are going to assume that the domain D is a polygon (if $d = 2$) or a polyhedron (if $d = 3$) so that it can be meshed exactly with cells having straight edges or planar faces, respectively, and we are going to assume that the above smoothness assumptions on the exact solution still hold true.

3 Discontinuous-Skeletal discretization

In this section, we present the setting for the Discontinuous-Skeletal discretization of the elliptic obstacle problem introduced in the previous section.

3.1 Discrete setting

We consider a sequence of refined meshes $(\mathcal{T}_h)_{h>0}$ where the parameter h denotes the mesh-size and goes to zero during the refinement process. For all $h > 0$, we assume that the mesh \mathcal{T}_h covers D exactly and consists of a finite collection of non-empty disjoint open polyhedral cells T such that $\bar{D} = \bigcup_{T \in \mathcal{T}_h} \bar{T}$ and $h = \max_{T \in \mathcal{T}_h} h_T$, where h_T is the diameter of T . The present Discontinuous-Skeletal methods can be deployed on meshes composed of triangular or quadrangular cells (if $d = 2$) and of tetrahedral or hexahedral cells (if $d = 3$), all having matching interfaces. In this situation, we assume that the mesh sequence $(\mathcal{T}_h)_{h>0}$ is shape-regular in the usual sense of Ciarlet.

More generally, it is possible to consider meshes having non-matching interfaces and cells of polyhedral shape. A closed subset F of \bar{D} is defined to be a mesh face if it is a subset of an affine hyperplane H_F with positive $(d - 1)$ -dimensional Hausdorff measure and if either of the following two statements holds true: (i) There exist $T_1(F)$ and $T_2(F)$ in \mathcal{T}_h such that $F = \partial T_1(F) \cap \partial T_2(F) \cap H_F$; in this case, the face F

is called an internal face; (ii) There exists $T(F) \in \mathcal{T}_h$ such that $F = \partial T(F) \cap \partial D \cap H_F$; in this case, the face F is called a boundary face. The collection of all the internal (resp., boundary) faces is denoted by \mathcal{F}_h^i (resp., \mathcal{F}_h^b), and we let $\mathcal{F}_h := \mathcal{F}_h^i \cup \mathcal{F}_h^b$. Let h_F denote the diameter of $F \in \mathcal{F}_h$. For each $T \in \mathcal{T}_h$, the set $\mathcal{F}_T := \{F \in \mathcal{F}_h \mid F \subset \partial T\}$ denotes the collection of all faces contained in ∂T , \mathbf{n}_T the unit outward normal to T , and we set $\mathbf{n}_{TF} := \mathbf{n}_{T|F}$ for all $F \in \mathcal{F}_T$. Following [23, Def. 1], we assume that the mesh sequence $(\mathcal{T}_h)_{h>0}$ is shape-regular in the sense that, for all $h > 0$, \mathcal{T}_h admits a matching simplicial submesh \mathfrak{T}_h (i.e., every cell and face of \mathfrak{T}_h is a subset of a cell and a face of \mathcal{T}_h , respectively) so that the mesh sequence $(\mathfrak{T}_h)_{h>0}$ is shape-regular in the usual sense and all the cells and faces of \mathfrak{T}_h have uniformly comparable diameter to the cell and face of \mathcal{T}_h to which they belong. For a shape-regular mesh sequence $(\mathcal{T}_h)_{h>0}$, the maximum number of faces of a mesh cell is uniformly bounded (see [22, Lemma 1.41]), i.e., there is a positive integer N_∂ , uniform with respect to h , such that

$$\max_{T \in \mathcal{T}_h} \text{card}(\mathcal{F}_T) \leq N_\partial \quad \forall h > 0. \quad (3.1)$$

Moreover, the following discrete trace inequality holds true, see [22, Lemma 1.46]:

$$\|q\|_F \leq C_{\text{tr}} h_F^{-\frac{1}{2}} \|q\|_T \quad \forall T \in \mathcal{T}_h, \forall F \in \mathcal{F}_T, \forall q \in \mathbb{P}_d^r(T), \quad (3.2)$$

where C_{tr} depends on the polynomial degree $r \geq 0$ but is uniform with respect to h . Henceforth, we use the notation C for a positive generic constant whose value can change at each occurrence but is independent of the mesh cell $T \in \mathcal{T}_h$ and of h . The value of C can depend on the shape-regularity of the mesh sequence and on the underlying polynomial degree.

3.2 Local reconstruction and stabilization operators

Let the polynomial degree $k \in \{0, 1\}$ be fixed. For all $T \in \mathcal{T}_h$, we define the local discrete space by

$$\hat{U}_T^k := \mathbb{P}_d^0(T) \times \mathbb{P}_{d-1}^k(\partial T), \quad (3.3)$$

where $\mathbb{P}_{d-1}^k(\partial T) := \times_{F \in \mathcal{F}_T} \mathbb{P}_{d-1}^k(F)$ is composed of piecewise polynomials of degree at most k on the faces composing the boundary of T . We represent a generic element $\hat{v}_T \in \hat{U}_T^k$ by $\hat{v}_T = (v_T, v_{\partial T})$ with $v_T \in \mathbb{P}_d^0(T)$ and $v_{\partial T} \in \mathbb{P}_{d-1}^k(\partial T)$. For all $T \in \mathcal{T}_h$, we define the local reconstruction operator $p_T^{k+1} : \hat{U}_T^k \rightarrow \mathbb{P}_d^{k+1}(T)$ so that, for all $\hat{v}_T = (v_T, v_{\partial T}) \in \hat{U}_T^k$,

$$(\nabla p_T^{k+1}(\hat{v}_T), \nabla w)_T = (\nabla v_T, \nabla w)_T + (v_{\partial T} - v_T, \nabla w \cdot \mathbf{n}_T)_{\partial T} \quad \forall w \in \mathbb{P}_d^{k+1}(T), \quad (3.4a)$$

$$(p_T^{k+1}(\hat{v}_T), 1)_T = (v_T, 1)_T. \quad (3.4b)$$

The volume term on the right-hand side of (3.4a) is zero since v_T is constant; we keep this term for the sake of consistency with the general setting from [25, 23]. Let π_T^0 be the L^2 -projection onto $\mathbb{P}_d^0(T)$ and let $\pi_{\partial T}^k$ be the L^2 -projection onto $\mathbb{P}_{d-1}^k(\partial T)$. We define the local stabilization operator $S_{\partial T}^k : \hat{U}_T^k \rightarrow \mathbb{P}_{d-1}^k(\partial T)$ such that, for all $\hat{v}_T = (v_T, v_{\partial T}) \in \hat{U}_T^k$, we have

$$S_{\partial T}^k(\hat{v}_T) := \pi_{\partial T}^k(v_{\partial T} - p_T^{k+1}(\hat{v}_T)) - \pi_T^0(v_T - p_T^{k+1}(\hat{v}_T))|_{\partial T}. \quad (3.5)$$

Notice that in the present setting, the second term on the right-hand side is a constant. Finally, the discrete counterpart of the local exact bilinear form $(\nabla w, \nabla v)_T$ is the local discrete bilinear form $a_T : \hat{U}_T^k \times \hat{U}_T^k \rightarrow \mathbb{R}$ defined by

$$a_T(\hat{w}_T, \hat{v}_T) := (\nabla p_T^{k+1}(\hat{w}_T), \nabla p_T^{k+1}(\hat{v}_T))_T + (\eta_{\partial T} S_{\partial T}^k(\hat{w}_T), S_{\partial T}^k(\hat{v}_T))_{\partial T}, \quad (3.6)$$

with the piecewise constant weight $\eta_{\partial T}$ defined on ∂T such that $\eta_{\partial T|F} = h_F^{-1}$ for all $F \in \mathcal{F}_T$.

Let us briefly outline the stability and approximation properties associated with the above operators. We equip the discrete space \hat{U}_T^k with the following seminorm:

For all $\hat{v}_T = (v_T, v_{\partial T}) \in \hat{U}_T^k$,

$$|\hat{v}_T|_{\hat{U}_T^k} := \|\eta_{\partial T}^{\frac{1}{2}}(v_{\partial T} - v_T)\|_{\partial T}. \quad (3.7)$$

Observe that $|\hat{v}_T|_{\hat{U}_T^k} = 0$ implies that $v_{\partial T}$ is constant on ∂T and equal to v_T .

Lemma 3.1 (Stability). *There exist positive constants C_1 and C_2 , uniform with respect to T and h , such that, for all $\hat{v}_T \in \hat{U}_T^k$,*

$$C_1 |\hat{v}_T|_{\hat{U}_T^k}^2 \leq a_T(\hat{v}_T, \hat{v}_T) \leq C_2 |\hat{v}_T|_{\hat{U}_T^k}^2. \quad (3.8)$$

Proof. The proof follows that of [25, Lemma 4]. We briefly sketch it for completeness since we are dealing here with different polynomial degrees for the face and the cell unknowns. Let $\hat{v}_T \in \hat{U}_T^k$. Invoking the triangle inequality, the regularity of the mesh sequence, the L^2 -stability of $\pi_{\partial T}^k$, and the approximation properties of π_T^0 , we infer that

$$\begin{aligned} |\hat{v}_T|_{\hat{U}_T^k} &\leq \|\eta_{\partial T}^{\frac{1}{2}} S_{\partial T}^k(\hat{v}_T)\|_{\partial T} + \|\eta_{\partial T}^{\frac{1}{2}} \pi_{\partial T}^k(p_T^{k+1}(\hat{v}_T) - \pi_T^0(p_T^{k+1}(\hat{v}_T)))\|_{\partial T} \\ &\leq \|\eta_{\partial T}^{\frac{1}{2}} S_{\partial T}^k(\hat{v}_T)\|_{\partial T} + Ch_T^{-1} \|p_T^{k+1}(\hat{v}_T) - \pi_T^0(p_T^{k+1}(\hat{v}_T))\|_T \\ &\leq \|\eta_{\partial T}^{\frac{1}{2}} S_{\partial T}^k(\hat{v}_T)\|_{\partial T} + C' \|\nabla p_T^{k+1}(\hat{v}_T)\|_T, \end{aligned}$$

which proves the leftmost bound in (3.8). Concerning the rightmost bound, we first observe that the definition (3.4a) of $p_T^{k+1}(\hat{v}_T)$ combined with the Cauchy–Schwarz inequality and the trace inequality (3.2) readily imply that $\|\nabla p_T^{k+1}(\hat{v}_T)\|_T \leq C |\hat{v}_T|_{\hat{U}_T^k}$. Moreover, invoking the same arguments as above implies that

$$\begin{aligned} \|\eta_{\partial T}^{\frac{1}{2}} S_{\partial T}^k(\hat{v}_T)\|_{\partial T} &\leq |\hat{v}_T|_{\hat{U}_T^k} + \|\eta_{\partial T}^{\frac{1}{2}} \pi_{\partial T}^k(p_T^{k+1}(\hat{v}_T) - \pi_T^0(p_T^{k+1}(\hat{v}_T)))\|_{\partial T} \\ &\leq |\hat{v}_T|_{\hat{U}_T^k} + C' \|\nabla p_T^{k+1}(\hat{v}_T)\|_T, \end{aligned}$$

and since we have already proved that $\|\nabla p_T^{k+1}(\hat{v}_T)\|_T \leq C |\hat{v}_T|_{\hat{U}_T^k}$, this concludes the proof. \square

We define the local reduction operator $\hat{I}_T^k : H^1(T) \rightarrow \hat{U}_T^k$ such that, for all $v \in H^1(T)$,

$$\hat{I}_T^k(v) := (\pi_T^0(v), \pi_{\partial T}^k(v)) \in \hat{U}_T^k. \quad (3.9)$$

Then, $p_T^{k+1} \circ \hat{I}_T^k : H^1(T) \rightarrow \mathbb{P}_d^{k+1}(T)$ acts as an approximation operator.

Lemma 3.2 (Approximation). *Let $s \geq 0$ and set $t := \min(k, s)$. There is C , uniform with respect to T and h , so that, for any $v \in H^{s+2}(T)$, the following holds true:*

$$\begin{aligned} \|v - p_T^{k+1}(\hat{I}_T^k(v))\|_T + h_T^{\frac{1}{2}} \|v - p_T^{k+1}(\hat{I}_T^k(v))\|_{\partial T} + h_T \|\nabla(v - p_T^{k+1}(\hat{I}_T^k(v)))\|_T \\ + h_T^{\frac{3}{2}} \|\nabla(v - p_T^{k+1}(\hat{I}_T^k(v)))\|_{\partial T} \leq Ch_T^{t+2} |v|_{H^{t+2}(T)}. \end{aligned} \quad (3.10)$$

Moreover, we have

$$\|\eta_{\partial T}^{\frac{1}{2}} S_{\partial T}^k(\hat{I}_T^k(v))\|_{\partial T} \leq Ch_T^{t+1} |v|_{H^{t+2}(T)}. \quad (3.11)$$

Proof. The proof of (3.10) is similar to [25, Lemma 3] (up to minor adaptations due to the different polynomial degrees for the face and the cell unknowns). The key observation is that $(\nabla(v - p_T^k(\hat{I}_T^k(v))), \nabla w)_T = 0$ for all $w \in \mathbb{P}_d^{k+1}(T)$, so that $\|\nabla(v - p_T^k(\hat{I}_T^k(v)))\|_T = \inf_{w \in \mathbb{P}_d^{k+1}(T)} \|\nabla(v - w)\|_T$. Concerning (3.11), we have

$$S_{\partial T}^k(\hat{I}_T^k(v)) = \pi_{\partial T}^k(v - p_T^{k+1}(\hat{I}_T^k(v))) - \pi_T^0(v - p_T^{k+1}(\hat{I}_T^k(v)))|_{\partial T}.$$

Therefore, proceeding as in [25, Eq. (45)], we use the triangle inequality, the stability of the L^2 -projectors, that $\eta_{\partial T}$ is piecewise constant, and the regularity of the mesh sequence to infer that

$$\begin{aligned} \|\eta_{\partial T}^{\frac{1}{2}} S_{\partial T}^k(\hat{I}_T^k(v))\|_{\partial T} &\leq \|\eta_{\partial T}^{\frac{1}{2}} \pi_{\partial T}^k(v - p_T^{k+1}(\hat{I}_T^k(v)))\|_{\partial T} + \|\eta_{\partial T}^{\frac{1}{2}} \pi_T^0(v - p_T^{k+1}(\hat{I}_T^k(v)))\|_{\partial T} \\ &\leq \|\eta_{\partial T}^{\frac{1}{2}}(v - p_T^{k+1}(\hat{I}_T^k(v)))\|_{\partial T} + Ch_T^{-1} \|\pi_T^0(v - p_T^{k+1}(\hat{I}_T^k(v)))\|_T \\ &\leq C' h_T^{-1} (h_T^{\frac{1}{2}} \|v - p_T^{k+1}(\hat{I}_T^k(v))\|_{\partial T} + \|v - p_T^{k+1}(\hat{I}_T^k(v))\|_T), \end{aligned}$$

and we conclude by invoking (3.10). \square

3.3 Discrete elliptic obstacle problem

The global discrete space is defined by

$$\hat{U}_h^k := \left(\times_{T \in \mathcal{T}_h} \mathbb{P}_d^0(T) \right) \times \left(\times_{F \in \mathcal{F}_h} \mathbb{P}_{d-1}^k(F) \right). \quad (3.12)$$

We use the notation $\hat{v}_h = ((v_T)_{T \in \mathcal{T}_h}, (v_F)_{F \in \mathcal{F}_h})$ to denote a generic element $\hat{v}_h \in \hat{U}_h^k$. For all $T \in \mathcal{T}_h$, we denote by $\hat{v}_T = (v_T, (v_F)_{F \in \mathcal{F}_T}) \in \hat{U}_T^k$ the components of \hat{v}_h attached to the mesh cell T and the faces composing its boundary. We define the global reduction operator $\hat{I}_h^k : H^1(D) \rightarrow \hat{U}_h^k$ such that, for all $v \in H^1(D)$,

$$\hat{I}_h^k(v) := ((\pi_T^0(v))_{T \in \mathcal{T}_h}, (\pi_F^k(v))_{F \in \mathcal{F}_h}). \quad (3.13)$$

Note that $\hat{I}_h^k(v)$ is well-defined since v is single-valued at all the internal faces of the mesh.

The global discrete bilinear form a_h on $\hat{U}_h^k \times \hat{U}_h^k$ is defined by

$$a_h(\hat{w}_h, \hat{v}_h) := \sum_{T \in \mathcal{T}_h} a_T(\hat{w}_T, \hat{v}_T) + \sum_{F \in \mathcal{F}_h^b} a_F^b(\hat{w}_{T(F)}, \hat{v}_{T(F)}), \quad (3.14)$$

with the Nitsche-type boundary penalty bilinear form [41] such that

$$a_F^b(\hat{w}_{T(F)}, \hat{v}_{T(F)}) := -(\nabla p_{T(F)}^{k+1}(\hat{w}_{T(F)}) \cdot \mathbf{n}_D, v_F)_F - (w_F, \nabla p_{T(F)}^{k+1}(\hat{v}_{T(F)}) \cdot \mathbf{n}_D)_F + \varsigma h_F^{-1} (w_F, v_F)_F, \quad (3.15)$$

where $\varsigma > 0$ is the boundary penalty parameter and \mathbf{n}_D is the unit outward normal to D . The linear form ℓ_h on \hat{U}_h^k is defined by

$$\ell_h(\hat{v}_h) := \sum_{T \in \mathcal{T}_h} (f, v_T)_T + \sum_{F \in \mathcal{F}_h^b} \ell_F^b(\hat{v}_{T(F)}), \quad (3.16)$$

with

$$\ell_F^b(\hat{v}_{T(F)}) := -(g, \nabla p_{T(F)}^{k+1}(\hat{v}_{T(F)}) \cdot \mathbf{n}_D)_F + \varsigma h_F^{-1} (g, v_F)_F. \quad (3.17)$$

Remark 3.3 (Dirichlet boundary conditions). Alternatively, one can also enforce Dirichlet boundary conditions strongly by setting the discrete unknowns attached to the boundary faces of the mesh equal to the L^2 -projection of the Dirichlet data onto $\mathbb{P}_{d-1}^k(F)$ for all $F \in \mathcal{F}_h^b$ and zeroing out the discrete test functions attached to the boundary faces of the mesh. In this case, the contribution of a_F^b is dropped from the right-hand side of (3.14) and that of ℓ_F^b is dropped from the right-hand side of (3.16). This is the approach we use in the numerical experiments reported below, but to allow for a bit more generality, we consider the above boundary-penalty method in the error analysis.

The discrete admissible set $\hat{\mathcal{K}}_h^k$ is defined by

$$\hat{\mathcal{K}}_h^k := \left\{ \hat{v}_h \in \hat{U}_h^k \mid (v_T, 1)_T \geq (\chi, 1)_T, \forall T \in \mathcal{T}_h \right\}. \quad (3.18)$$

Notice that the constraint is enforced on the cell unknowns. The discrete elliptic obstacle problem consists of finding $\hat{u}_h \in \hat{\mathcal{K}}_h^k$ such that

$$a_h(\hat{u}_h, \hat{v}_h - \hat{u}_h) \geq \ell_h(\hat{v}_h - \hat{u}_h) \quad \forall \hat{v}_h \in \hat{\mathcal{K}}_h^k. \quad (3.19)$$

Equivalently, \hat{u}_h minimizes over $\hat{\mathcal{K}}_h^k$ the discrete functional $\frac{1}{2} a_h(\hat{v}_h, \hat{v}_h) - \ell_h(\hat{v}_h)$. In order to establish the well-posedness of the discrete problem (3.19), we study the coercivity and boundedness of the discrete bilinear form a_h on $\hat{U}_h^k \times \hat{U}_h^k$. To this purpose, we equip the space \hat{U}_h^k with the following norm:

$$\|\hat{v}_h\|_{\hat{U}_h^k}^2 := \sum_{T \in \mathcal{T}_h} |\hat{v}_T|_{\hat{U}_T^k}^2 + \sum_{F \in \mathcal{F}_h^b} h_F^{-1} \|v_F\|_F^2. \quad (3.20)$$

Lemma 3.4. *Assume that the boundary penalty parameter is such that $\varsigma > \frac{1}{4} N_\partial C_{\text{tr}}^2$ where N_∂ is defined by (3.1) and C_{tr} by (3.2). Then, there exists two positive constants α and ξ , uniform with respect to h , such that, for all $\hat{v}_h, \hat{w}_h \in \hat{U}_h^k$,*

$$a_h(\hat{v}_h, \hat{v}_h) \geq \alpha \|\hat{v}_h\|_{\hat{U}_h^k}^2, \quad (3.21a)$$

$$|a_h(\hat{v}_h, \hat{w}_h)| \leq \xi \|\hat{w}_h\|_{\hat{U}_h^k} \|\hat{v}_h\|_{\hat{U}_h^k}. \quad (3.21b)$$

Proof. The coercivity property (3.21a) follows from the left bound in (3.8) and classical techniques for Nitsche's boundary penalty method, see, e.g., [22, Lemma 4.12] in the context of discontinuous Galerkin methods and [26, Lemma 7] in the context of HHO methods. The boundedness property (3.21b) follows from the Cauchy–Schwarz inequality, the right bound in (3.8), and by invoking the discrete trace inequality (3.2) to bound the first two terms composing a_h^b . \square

Corollary 3.5 (Well-posedness). *Assume that $\varsigma > \frac{1}{4}N_\delta C_{\text{tr}}^2$. There exists a unique $\hat{u}_h \in \hat{\mathcal{K}}_h^k$ solving the discrete elliptic obstacle problem (3.19).*

Proof. The discrete admissible set $\hat{\mathcal{K}}_h^k$ is nonempty since $\hat{I}_h^k(u) \in \hat{\mathcal{K}}_h^k$. Moreover, $\hat{\mathcal{K}}_h^k$ is a closed convex subset of \hat{U}_h^k . We can then invoke the Browder–Stampacchia Lemma 2.1 together with the coercivity and boundedness result from Lemma 3.4 to conclude. \square

4 Error analysis

In this section, we state and prove our main result, that is, an energy-error estimate for the Discontinuous-Skeletal method with $k \in \{0, 1\}$. The estimate is optimal up to the regularity of the exact solution if $k = 1$, whereas if $k = 0$, the estimate is still optimal concerning the differentiability index of the exact solution, but requires a somewhat stronger assumption on the integrability index since we essentially require that $u \in W^{2,p}(D)$ with p large enough instead of just $u \in H^2(D)$ (see also Remark 4.2 below).

Theorem 4.1 (Energy-error estimate). *Let u be the exact solution solving (2.3) and let \hat{u}_h be the discrete solution solving (3.19). Let \hat{I}_h^k be the global reduction operator defined by (3.13). If $k = 1$, let $\epsilon \in (0, \frac{1}{2}]$, set $r = \frac{3}{2} - \epsilon$, and assume that $u \in H^{1+r}(D) = H^{\frac{5}{2}-\epsilon}(D)$, $(u - \chi) \in W^{2+\frac{1}{p}-\frac{\epsilon}{2},p}(D)$ with $p = \frac{2(d-1)}{\epsilon} \in (1, \infty)$, and $\lambda := -f - \Delta u \in W^{1-\epsilon,1}(D)$. If $k = 0$, set $r = 1$, let $\tau \in (0, 1)$, and assume that $u \in H^{1+r}(D) = H^2(D)$, $(u - \chi) \in W^{2,p}(D)$ with $p = \frac{d}{\tau} \in (1, \infty)$, and $\lambda := -f - \Delta u \in W^{\tau,1}(D)$. Then, there is C , uniform with respect to h , such that the following holds true:*

$$\|\hat{I}_h^k(u) - \hat{u}_h\|_{\hat{U}_h^k} \leq C(|u|_{H^{1+r}(D)} + \Phi_{u,\lambda})h^r, \quad (4.1)$$

where

$$\Phi_{u,\lambda} = \begin{cases} \|u - \chi\|_{W^{2+\frac{1}{p}-\frac{\epsilon}{2},p}(D)}^{\frac{1}{2}} |\lambda|_{W^{1-\epsilon,1}(D)}^{\frac{1}{2}} & \text{if } k = 1, \\ \|u - \chi\|_{W^{2,p}(D)}^{\frac{1}{2}} |\lambda|_{W^{\tau,1}(D)}^{\frac{1}{2}} & \text{if } k = 0. \end{cases} \quad (4.2)$$

Moreover, we also have

$$\left(\sum_{T \in \mathcal{T}_h} \|\nabla(u - p_T^{k+1}(\hat{u}_T))\|_T^2 + \sum_{F \in \mathcal{F}_h^b} h_F^{-1} \|u - u_F\|_F^2 \right)^{\frac{1}{2}} \leq C(|u|_{H^{1+r}(D)} + \Phi_{u,\lambda})h^r. \quad (4.3)$$

Proof. Let us set $\hat{v}_h := \hat{I}_h^k(u) - \hat{u}_h \in \hat{U}_h^k$. Using the discrete coercivity property (3.21a) and the discrete variational inequality (3.19) together with $\hat{I}_h^k(u) \in \hat{\mathcal{K}}_h^k$, we find that

$$\begin{aligned} \alpha \|\hat{I}_h^k(u) - \hat{u}_h\|_{\hat{U}_h^k}^2 &\leq a_h(\hat{I}_h^k(u) - \hat{u}_h, \hat{I}_h^k(u) - \hat{u}_h) \\ &\leq a_h(\hat{I}_h^k(u), \hat{I}_h^k(u) - \hat{u}_h) - \ell_h(\hat{I}_h^k(u) - \hat{u}_h) \\ &= a_h(\hat{I}_h^k(u), \hat{v}_h) - \ell_h(\hat{v}_h) \\ &= a_h(\hat{I}_h^k(u), \hat{v}_h) + \sum_{T \in \mathcal{T}_h} (\Delta u, v_T)_T - \sum_{F \in \mathcal{F}_h^b} \ell_F^b(\hat{v}_{T(F)}) + \sum_{T \in \mathcal{T}_h} (\lambda, \pi_T^0(u) - u_T)_T, \end{aligned}$$

where we used $\lambda = -f - \Delta u$ and that the cell component of \hat{v}_h attached to $T \in \mathcal{T}_h$ is $v_T = \pi_T^0(u) - u_T$. Let us define $\mathcal{T}_h^n := \{T \in \mathcal{T}_h \mid u > \chi \text{ on } T\}$ (collecting the non-contact cells), $\mathcal{T}_h^c := \{T \in \mathcal{T}_h \mid u \equiv \chi \text{ on } T\}$ (collecting the contact cells), and $\mathcal{T}_h^f := \mathcal{T}_h \setminus (\mathcal{T}_h^n \cup \mathcal{T}_h^c)$ (collecting the free-boundary cells). Note that $\lambda \equiv 0$ on any $T \in \mathcal{T}_h^n$ owing to (2.5b). Therefore, we have

$$\sum_{T \in \mathcal{T}_h} (\lambda, \pi_T^0(u) - u_T)_T = \sum_{T \in \mathcal{T}_h^c} (\lambda, \pi_T^0(u) - u_T)_T + \sum_{T \in \mathcal{T}_h^f} (\lambda, \pi_T^0(u) - u_T)_T.$$

Moreover, for all $T \in \mathcal{T}_h^c$, we have $\pi_T^0(u) = \pi_T^0(\chi)$, and hence

$$(\lambda, \pi_T^0(u) - u_T)_T = (\lambda, \pi_T^0(\chi) - u_T)_T \leq 0,$$

recalling that $u_T \geq \pi_T^0(\chi)$ since $\hat{u}_h \in \hat{\mathcal{K}}_h^k$ and that $\lambda \geq 0$ on D owing to (2.5a). As a result, we have

$$\alpha \|\hat{I}_h^k(u) - \hat{u}_h\|_{\hat{U}_h^k}^2 \leq a_h(\hat{I}_h^k(u), \hat{v}_h) + \sum_{T \in \mathcal{T}_h} (\Delta u, v_T)_T - \sum_{F \in \mathcal{F}_h^b} \ell_F^b(\hat{v}_{T(F)}) + \sum_{T \in \mathcal{T}_h^f} (\lambda, \pi_T^0(u) - u_T)_T.$$

The first three terms on the right hand side are estimated in Lemma 4.3 below, and the last term is estimated in Lemma 4.4 below. This proves (4.1). Finally, the bound (4.3) follows from (4.1) by invoking the rightmost bound in (3.8), the triangle inequality, and the bound (3.10) on $\nabla(u - p_T^{k+1}(\hat{I}_T^k(u)))$ with $s = t = \frac{1}{2} - \epsilon \geq 0$ if $k = 1$ and $s = t = 0$ if $k = 0$. \square

Remark 4.2 (Regularity for $k = 0$). The regularity requirement $u \in W^{2,p}(D)$ with $p = \frac{d}{\tau}$ introduced in Theorem 4.1 for $k = 0$ can be reduced to $u \in H^2(D)$ provided one uses a Discontinuous-Skeletal method with affine cell unknowns on simplicial meshes and one enforces the obstacle constraint on the cell unknowns with respect to the linear Lagrange interpolate of the obstacle function. Details are omitted for brevity.

Lemma 4.3 (Consistency error on differential operator). *Let r be as in Theorem 4.1 and assume that the exact solution u is in $H^{1+r}(\Omega)$. There is C , uniform with respect to h , such that the following holds true for all $\hat{v}_h \in \hat{U}_h^k$:*

$$\left| a_h(\hat{I}_h^k(u), \hat{v}_h) + \sum_{T \in \mathcal{T}_h} (\Delta u, v_T)_T - \sum_{F \in \mathcal{F}_h^b} \ell_F^b(\hat{v}_{T(F)}) \right| \leq Ch^r |u|_{H^{1+r}(\Omega)} \|\hat{v}_h\|_{\hat{U}_h^k}.$$

Proof. The proof follows along the lines of [26, Sect. 6.2]; we sketch it for completeness. Re-organizing the various terms, we have

$$a_h(\hat{I}_h^k(u), \hat{v}_h) + \sum_{T \in \mathcal{T}_h} (\Delta u, v_T)_T - \sum_{F \in \mathcal{F}_h^b} \ell_F^b(\hat{v}_{T(F)}) = A_1 + A_2 + A_3,$$

where

$$\begin{aligned} A_1 &= \sum_{T \in \mathcal{T}_h} (\nabla p_T^{k+1}(\hat{I}_T^k(u)), \nabla p_T^{k+1}(\hat{v}_T))_T + (\Delta u, v_T)_T - \sum_{F \in \mathcal{F}_h^b} (\nabla p_{T(F)}^{k+1}(\hat{I}_{T(F)}^k(u)) \cdot \mathbf{n}_D, v_F)_F, \\ A_2 &= \sum_{T \in \mathcal{T}_h} (\eta_{\partial T} S_{\partial T}^k(\hat{I}_T^k(u)), S_{\partial T}^k(\hat{v}_T))_{\partial T}, \\ A_3 &= \sum_{F \in \mathcal{F}_h^b} -(\pi_F^k(u) - g, \nabla p_{T(F)}^{k+1}(\hat{v}_{T(F)}) \cdot \mathbf{n}_D)_F + \varsigma h_F^{-1} (\pi_F^k(u) - g, v_F)_F. \end{aligned}$$

Using the definition of p_T^{k+1} , integrating by parts the term $(\Delta u, v_T)_T$, and since the normal component of ∇u is single-valued across the mesh internal faces, we infer that

$$A_1 = \sum_{T \in \mathcal{T}_h} (\nabla(u - p_T^{k+1}(\hat{I}_T^k(u))) \cdot \mathbf{n}_T, v_{\partial T} - v_T)_{\partial T} + \sum_{F \in \mathcal{F}_h^b} (\nabla(u - p_{T(F)}^{k+1}(\hat{I}_{T(F)}^k(u))) \cdot \mathbf{n}_D, v_F)_F.$$

We can now use the bound (3.10) on $(u - p_T^{k+1}(\hat{I}_T^k(u)))$ where we set $s = r - 1$ so that $t = \min(k, s) = s = r - 1$ whether $k = 1$ or $k = 0$. Using the Cauchy-Schwarz inequality and the definition of the $\|\cdot\|_{\hat{U}_h^k}$ norm, we then obtain that $|A_1| \leq Ch^{t+1} |u|_{H^{t+2}(\Omega)} \|\hat{v}_h\|_{\hat{U}_h^k}$. Furthermore, since $\|\eta_{\partial T}^{\frac{1}{2}} S_{\partial T}^k(\hat{v}_T)\|_{\partial T} \leq C |\hat{v}_T|_{\hat{U}_T^k}$ for all $T \in \mathcal{T}_h$, the Cauchy-Schwarz inequality and the bound (3.11) on $\|\eta_{\partial T}^{\frac{1}{2}} S_{\partial T}^k(\hat{I}_T^k(u))\|_{\partial T}$ imply that $|A_2| \leq Ch^{t+1} |u|_{H^{t+2}(\Omega)} \|\hat{v}_h\|_{\hat{U}_h^k}$. Finally, since $\nabla p_{T(F)}^{k+1}(\hat{v}_{T(F)}) \cdot \mathbf{n}_D$ and v_F are polynomials of order at most k on F , we have $A_3 = 0$. \square

Lemma 4.4 (Consistency error on Lagrange multiplier). *Let p and $\Phi_{u,\lambda}$ be as in Theorem 4.1. There is C , uniform with respect to h , such that the following holds true:*

$$\sum_{T \in \mathcal{T}_h^f} (\lambda, \pi_T^0(u) - u_T)_T \leq C \Phi_{u,\lambda} h^r.$$

Proof. Let $T \in \mathcal{T}_h^f$. Then, using (2.5c), we infer that

$$(\lambda, \pi_T^0(u) - u_T)_T = (\lambda, \pi_T^0(u) - u + \chi - \pi_T^0(\chi) + \pi_T^0(\chi) - u_T)_T.$$

Since $(\lambda, \pi_T^0(\chi) - u_T)_T \leq 0$, we obtain

$$\begin{aligned} (\lambda, \pi_T^0(u) - u_T)_T &\leq (\lambda, \pi_T^0(u - \chi) - (u - \chi))_T = (\lambda - \pi_T^0(\lambda), \pi_T^0(u - \chi) - (u - \chi))_T \\ &\leq \|\lambda - \pi_T^0(\lambda)\|_{L^1(T)} \|(u - \chi) - \pi_T^0(u - \chi)\|_{L^\infty(T)}. \end{aligned} \quad (4.4)$$

(1) The case $k = 1$. The approximation properties of π_T^0 imply that

$$\|\lambda - \pi_T^0(\lambda)\|_{L^1(T)} \leq Ch_T^{1-\epsilon} |\lambda|_{W^{1-\epsilon,1}(T)}. \quad (4.5)$$

Furthermore, we also have

$$\|(u - \chi) - \pi_T^0(u - \chi)\|_{L^\infty(T)} \leq Ch_T |u - \chi|_{W^{1,\infty}(T)}. \quad (4.6)$$

The definition of p implies that $\alpha := 1 - \frac{d-1}{p} - \frac{\epsilon}{2} = 1 - \epsilon > 0$. Moreover, by assumption, we have $(u - \chi) \in W^{2+\frac{1}{p}-\frac{\epsilon}{2},p}(D)$. Then, the Sobolev Embedding Theorem implies that $\nabla(u - \chi) \in C^{0,\alpha}(\bar{D})$. Since $T \in \mathcal{T}_h^f$, there is a point $x^* \in T$ such that $\nabla(u - \chi)(x^*) = 0$ [45] and hence, for any $x \in T$, we have

$$|\nabla(u - \chi)(x)| \leq C|x - x^*|^\alpha \|u - \chi\|_{W^{2+\frac{1}{p}-\frac{\epsilon}{2},p}(D)} \leq Ch_T^\alpha \|u - \chi\|_{W^{2+\frac{1}{p}-\frac{\epsilon}{2},p}(D)}.$$

Therefore, we have

$$|u - \chi|_{W^{1,\infty}(T)} \leq Ch_T^\alpha \|u - \chi\|_{W^{2+\frac{1}{p}-\frac{\epsilon}{2},p}(D)}. \quad (4.7)$$

Using (4.7) in (4.6), we obtain

$$\|(u - \chi) - \pi_T^0(u - \chi)\|_{L^\infty(T)} \leq Ch_T^{1+\alpha} \|u - \chi\|_{W^{2+\frac{1}{p}-\frac{\epsilon}{2},p}(D)}. \quad (4.8)$$

Substituting (4.5) and (4.8) in (4.4) and summing over all $T \in \mathcal{T}_h^f$, we find that

$$\begin{aligned} \sum_{T \in \mathcal{T}_h^f} (\lambda, \pi_T^0(u) - u_T)_T &\leq Ch^{2+\alpha-\epsilon} \|u - \chi\|_{W^{2+\frac{1}{p}-\frac{\epsilon}{2},p}(D)} \sum_{T \in \mathcal{T}_h^f} |\lambda|_{W^{1-\epsilon,1}(T)} \\ &\leq Ch^{3-2\epsilon} \|u - \chi\|_{W^{2+\frac{1}{p}-\frac{\epsilon}{2},p}(D)} |\lambda|_{W^{1-\epsilon,1}(D)} = Ch^{3-2\epsilon} \Phi_{u,\lambda}, \end{aligned}$$

since $2 + \alpha - \epsilon = 3 - \frac{d-1}{p} - \frac{3\epsilon}{2} = 3 - 2\epsilon$. This completes the proof for $k = 1$.

(2) The case $k = 0$. Using the approximation properties of π_T^0 , we have

$$\|\lambda - \pi_T^0(\lambda)\|_{L^1(T)} \leq Ch_T^\tau |\lambda|_{W^{\tau,1}(T)}, \quad (4.9)$$

and we also have

$$\|(u - \chi) - \pi_T^0(u - \chi)\|_{L^\infty(T)} \leq Ch_T |u - \chi|_{W^{1,\infty}(T)}.$$

Since $\tau \in (0,1)$ and $p = \frac{d}{\tau}$, we have $\gamma := 1 - \frac{d}{p} = 1 - \tau > 0$. Moreover, by assumption, we have $(u - \chi) \in W^{2,p}(D)$. Then, the Sobolev Embedding Theorem implies that $\nabla(u - \chi) \in C^{0,\gamma}(\bar{D})$. Proceeding as above for $k = 1$, we infer that

$$\|(u - \chi) - \pi_T^0(u - \chi)\|_{L^\infty(T)} \leq Ch_T^{1+\gamma} \|u - \chi\|_{W^{2,p}(D)}. \quad (4.10)$$

Using (4.9) and (4.10) in (4.4) and summing over all $T \in \mathcal{T}_h^f$, we find that

$$\begin{aligned} \sum_{T \in \mathcal{T}_h^f} (\lambda, \pi_T^0(u) - u_T)_T &\leq Ch^{1+\gamma+\tau} \|u - \chi\|_{W^{2,p}(D)} \sum_{T \in \mathcal{T}_h^f} |\lambda|_{W^{\tau,1}(T)} \\ &\leq Ch^2 \|u - \chi\|_{W^{2,p}(D)} |\lambda|_{W^{\tau,1}(D)} = Ch^2 \Phi_{u,\lambda}, \end{aligned}$$

since $1 + \gamma + \tau = 2 - \frac{d}{p} + \tau = 2$. This completes the proof for $k = 0$. \square

5 Numerical experiments

In this section, we briefly review some implementation aspects of the present Discontinuous-Skeletal methods applied to elliptic obstacle problems, and we illustrate the above theoretical results on two- and three-dimensional test cases from [42].

5.1 Implementation aspects

We implement Dirichlet boundary conditions strongly (see Remark 3.3). The standard HHO matrix associated with the bilinear form $a_h(\hat{w}_h, \hat{v}_h) = \sum_{T \in \mathcal{T}_h} a_T(\hat{w}_T, \hat{v}_T)$ is denoted $\mathbf{A} \in \mathbb{R}^{N_h^k \times N_h^k}$ with $N_h^k := |\mathcal{T}_h| + \binom{k+d-1}{d-1} |\mathcal{F}_h^i|$ (recall that the cell unknowns are constant in each mesh cell), and the load vector associated with the linear form $\ell_h(\hat{v}_h) = \sum_{T \in \mathcal{T}_h} (f, v_T)_T$ is denoted $\mathbf{b} \in \mathbb{R}^{N_h^k}$. For any vector $\boldsymbol{\alpha} \in \mathbb{R}^{N_h^k}$, we denote $\alpha_T \in \mathbb{R}$ its components attached to the mesh cell $T \in \mathcal{T}_h$ and $(\alpha_{F,n})_{0 \leq n < \binom{k+d-1}{d-1}}$ its components attached to the internal face $F \in \mathcal{F}_h^i$ of the mesh.

The numerical solution of the discrete elliptic obstacle problem (3.19) is based on the primal-dual active set method (see [37]). Let $m \geq 0$ be the iteration counter. For all $m \geq 0$, we are looking for the solution vector $\boldsymbol{\alpha}^m \in \mathbb{R}^{N_h^k}$ and the Lagrange multiplier vector $\boldsymbol{\beta}^m \in \mathbb{R}^{N_h^k}$ (note that $\boldsymbol{\beta}^m$ is actually a discrete counterpart of the function $-\lambda$ considered in the previous section). Since the constraint is enforced on the cell unknowns, the components of $\boldsymbol{\beta}$ attached to the internal faces of the mesh are always zero. Moreover, since the cell unknowns are constant in each mesh cell, the primal-dual active set method leads to a partition of the mesh cells into active and inactive ones; specifically, we consider the subsets $\mathcal{T}_A^m := \{T \in \mathcal{T}_h \mid \beta_T^m + c(\alpha_T^m - \gamma_T) < 0\}$ and $\mathcal{T}_I^m := \mathcal{T} \setminus \mathcal{T}_A^m$, where $c > 0$ is a numerical weighting parameter and $\gamma_T = \frac{1}{|T|} \int_T \chi$ for all $T \in \mathcal{T}_h$. For all $m \geq 1$, given the pair $(\boldsymbol{\alpha}^{m-1}, \boldsymbol{\beta}^{m-1}) \in \mathbb{R}^{N_h^k} \times \mathbb{R}^{N_h^k}$ and the resulting partition $(\mathcal{T}_A^{m-1}, \mathcal{T}_I^{m-1})$ of \mathcal{T}_h , we solve the following (nonsymmetric) linear system:

$$\begin{cases} \mathbf{A}\boldsymbol{\alpha}^m + \boldsymbol{\beta}^m = \mathbf{b} \\ \alpha_T^m = \gamma_T \quad \forall T \in \mathcal{T}_A^{m-1}, \\ \beta_T^m = 0, \quad \forall T \in \mathcal{T}_I^{m-1}. \end{cases} \quad (5.1)$$

The iteration is started with $\boldsymbol{\alpha}^0 = \mathbf{0}$, $\beta_T^0 = -1$ for all $T \in \mathcal{T}_h$, and the stopping criterion is $\|\boldsymbol{\alpha}^{m+1} - \boldsymbol{\alpha}^m\|_{\ell^2(\mathbb{R}^{N_h^k})} < 10^{-6}$. The weighting parameter is set to $c = 1$. The above linear system is solved using the PARDISO direct linear solver included in the Intel MKL library. For further insight into the implementation of Discontinuous-Skeletal methods, the reader is referred to [18]. The open-source template library DiSk++ is available at <https://github.com/datafl4sh/diskpp> (for a fast-prototyping environment, limited to simple 2D meshes, see also the library ProtoN available at <https://github.com/datafl4sh/ProtoN>).

5.2 2D and 3D test cases

In 2D, we consider the square domain $\Omega = (-1, 1)^2$ and the obstacle function $\chi = 0$. We prescribe a contact radius $r_0 = 0.7$ and, setting $r^2 = x^2 + y^2$, we take the load function

$$f(x, y) := \begin{cases} -4(4r^2 - 2r_0^2) & \text{if } r > r_0, \\ -8r_0^2(1 - r^2 + r_0^2) & \text{if } r \leq r_0. \end{cases} \quad (5.2)$$

It can be shown that the exact solution solving (2.3) is $u(x, y) = \max(r^2 - r_0^2, 0)^2$. Isocontours of the exact solution obtained using one of the hexagonal meshes from our tests are displayed in Figure 1. In 3D, we consider the cubic domain $\Omega = (0, 1)^3$ and the obstacle function $\chi = 0$. We prescribe again a contact radius $r_0 = 0.7$ and, setting $r^2 = x^2 + y^2 + z^2$, we take the load function

$$f(x, y, z) := \begin{cases} -4(5r^2 - 3r_0^2) & \text{if } r > r_0, \\ -8r_0^2(1 - r^2 + r_0^2) & \text{if } r \leq r_0, \end{cases} \quad (5.3)$$

so that the exact solution solving (2.3) is $u(x, y, z) = \max(r^2 - r_0^2, 0)^2$.

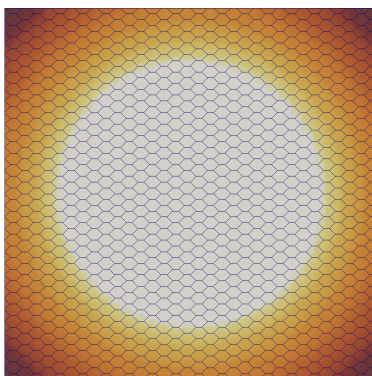


Figure 1: Isocontours of the 2D exact solution obtained on one of the hexagonal meshes.

The computations are run on six types of mesh sequences (each obtained by successive uniform refinements from an initial coarse mesh). In 2D, we consider triangular, square Cartesian, and hexagonal mesh sequences, whereas in 3D, we consider tetrahedral, cubic Cartesian, and hexagonal-based-prismatic mesh sequences (this last mesh sequence corresponds to the set “F” of the FVCA6 benchmark [31]). The energy errors and convergence orders are reported in Table 1 for triangular and tetrahedral mesh sequences, in Table 2 for square and cubic Cartesian mesh sequences, and in Table 3 for hexagonal and hexagonal-based-prismatic mesh sequences. A summary of the results is presented in Figure 2. In all cases, we observe that the reported results match the theoretical predictions from the analysis.

Table 1: Errors and convergence rates on 2D triangular (left) and 3D tetrahedral meshes (right).

| 2D (triangles) | | | | | 3D (tetrahedra) | | | | |
|----------------|---------|------|---------|------|-----------------|---------|------|---------|------|
| h | $k = 0$ | | $k = 1$ | | h | $k = 0$ | | $k = 1$ | |
| | error | rate | error | rate | | error | rate | error | rate |
| 3.10e-2 | 6.50e-1 | – | 2.64e-2 | – | 2.73e-2 | 1.59e0 | – | 1.03e-1 | – |
| 1.55e-2 | 3.29e-1 | 0.98 | 8.29e-3 | 1.67 | 1.36e-2 | 7.56e-1 | 1.07 | 2.58e-2 | 1.98 |
| 7.76e-3 | 1.65e-1 | 0.99 | 2.60e-3 | 1.67 | 1.09e-2 | 6.05e-1 | 1.03 | 1.69e-2 | 1.95 |
| 3.88e-3 | 8.27e-2 | 1.00 | 8.92e-4 | 1.54 | 8.61e-3 | 4.79e-1 | 0.98 | 1.09e-2 | 1.86 |
| 1.94e-3 | 4.14e-2 | 1.00 | 3.07e-4 | 1.54 | 6.87e-3 | 3.83e-1 | 0.99 | 7.08e-3 | 1.89 |

Table 2: Errors and convergence rates on 2D (left) and 3D (right) Cartesian meshes.

| 2D (squares) | | | | | 3D (cubes) | | | | |
|--------------|---------|------|---------|------|------------|---------|------|---------|------|
| h | $k = 0$ | | $k = 1$ | | h | $k = 0$ | | $k = 1$ | |
| | error | rate | error | rate | | error | rate | error | rate |
| 6.25e-2 | 2.26e0 | – | 1.98e-1 | – | 4.17e-2 | 2.10e0 | – | 1.59e-1 | – |
| 3.13e-2 | 1.28e0 | 0.82 | 5.88e-2 | 1.75 | 2.08e-2 | 1.09e0 | 0.94 | 4.57e-2 | 1.79 |
| 1.56e-2 | 6.50e-1 | 0.98 | 1.72e-2 | 1.78 | 1.04e-2 | 5.54e-1 | 0.98 | 1.25e-2 | 1.88 |
| 7.81e-3 | 3.26e-1 | 0.99 | 5.30e-3 | 1.70 | 5.21e-3 | 2.78e-1 | 0.99 | 3.43e-3 | 1.86 |
| 3.91e-3 | 1.63e-1 | 1.00 | 1.68e-3 | 1.65 | 2.60e-3 | 1.39e-1 | 1.00 | 9.89e-4 | 1.79 |

Table 3: Errors and convergence rates on 2D hexagonal (left) and 3D prismatic meshes (right).

| 2D (hexagons) | | | | | 3D (hexagonal-based prisms) | | | | |
|---------------|---------|------|---------|------|-----------------------------|---------|------|---------|------|
| h | $k = 0$ | | $k = 1$ | | h | $k = 0$ | | $k = 1$ | |
| | error | rate | error | rate | | error | rate | error | rate |
| 1.31e-1 | 2.73e0 | — | 5.50e-1 | — | 2.00e-2 | 9.37e-1 | — | 3.30e-2 | — |
| 6.53e-2 | 2.25e0 | 0.28 | 1.72e-1 | 1.67 | 1.01e-2 | 4.94e-1 | 0.94 | 9.66e-3 | 1.80 |
| 3.27e-2 | 1.32e0 | 0.76 | 4.92e-2 | 1.81 | 6.76e-3 | 3.35e-1 | 0.97 | 4.57e-3 | 1.87 |
| 1.63e-2 | 7.01e-1 | 0.92 | 1.51e-2 | 1.71 | 5.08e-3 | 2.53e-1 | 0.98 | 2.68e-3 | 1.86 |
| 8.16e-3 | 3.60e-1 | 0.96 | 4.82e-3 | 1.65 | | | | | |

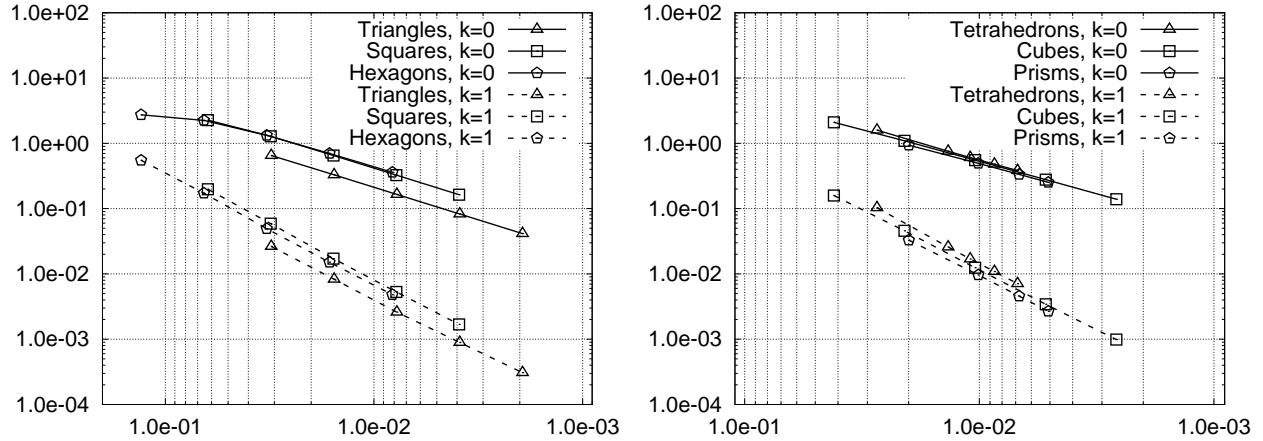


Figure 2: Summary of the convergence results for the 2D (left) and 3D (right) test cases. The mesh size is on the horizontal axis, and the energy error on the vertical axis. Solid lines show the results for $k = 0$, and dashed lines for $k = 1$.

References

- [1] M. Abbas, A. Ern, and N. Pignet. Hybrid High-Order methods for finite deformations of hyperelastic materials. *Comput. Mech.*, 2017. In press, available at <http://arxiv.org/abs/1709.03747>.
- [2] P. F. Antonietti, L. Beirão da Veiga, and M. Verani. A mimetic discretization of elliptic obstacle problems. *Math. Comp.*, 82(283):1379–1400, 2013.
- [3] B. Ayuso de Dios, K. Lipnikov, and G. Manzini. The nonconforming virtual element method. *ESAIM: Math. Model. Numer. Anal. (M2AN)*, 50(3):879–904, 2016.
- [4] Z. Belhachmi and F. B. Belgacem. Quadratic finite element approximation of the Signorini problem. *Math. Comp.*, 72(241):83–104, 2003.
- [5] F. Ben Belgacem. Numerical simulation of some variational inequalities arisen from unilateral contact problems by the finite element methods. *SIAM J. Numer. Anal.*, 37(4):1198–1216, 2000.
- [6] J. Bonelle and A. Ern. Analysis of compatible discrete operator schemes for elliptic problems on polyhedral meshes. *ESAIM Math. Model. Numer. Anal.*, 48(2):553–581, 2014.
- [7] M. Botti, D. A. Di Pietro, and P. Sochala. A Hybrid High-Order method for nonlinear elasticity. *SIAM J. Numer. Anal.*, 55(6):2687–2717, 2017.
- [8] S. C. Brenner, L.-Y. Sung, H. Zhang, and Y. Zhang. A quadratic C^0 interior penalty method for the displacement obstacle problem of clamped Kirchhoff plates. *SIAM J. Numer. Anal.*, 50(6):3329–3350, 2012.
- [9] S. C. Brenner, L.-Y. Sung, and Y. Zhang. Finite element methods for the displacement obstacle problem of clamped plates. *Math. Comp.*, 81(279):1247–1262, 2012.

- [10] H. Brezis. Seuil de régularité pour certains problèmes unilatéraux. *C. R. Acad. Sci. Paris Sér. A-B*, 273:A35–A37, 1971.
- [11] F. Brezzi, W. W. Hager, and P.-A. Raviart. Error estimates for the finite element solution of variational inequalities. *Numer. Math.*, 28(4):431–443, 1977.
- [12] F. Brezzi, K. Lipnikov, and M. Shashkov. Convergence of the mimetic finite difference method for diffusion problems on polyhedral meshes. *SIAM J. Numer. Anal.*, 43(5):1872–1896, 2005.
- [13] F. Brezzi, K. Lipnikov, M. Shashkov, and V. Simoncini. A new discretization methodology for diffusion problems on generalized polyhedral meshes. *Comput. Methods Appl. Mech. Engrg.*, 196(37-40):3682–3692, 2007.
- [14] F. Browder. On the unification of the calculus of variations and the theory of monotone non linear operators in Banach spaces. *Proc. Nat. Acad. Sci. U.S.A.*, 56:1080–1086, 1966.
- [15] E. Burman, P. Hansbo, and M. G. Larson. The penalty-free Nitsche method and nonconforming finite elements for the Signorini problem. *SIAM J. Numer. Anal.*, 55(6):2523–2539, 2017.
- [16] C. Carstensen and K. Köhler. Nonconforming FEM for the obstacle problem. *IMA J. Numer. Anal.*, 37(1):64–93, 2017.
- [17] F. Chouly and P. Hild. A Nitsche-based method for unilateral contact problems: numerical analysis. *SIAM J. Numer. Anal.*, 51(2):1295–1307, 2013.
- [18] M. Cicuttin, D. A. Di Pietro, and A. Ern. Implementation of Discontinuous Skeletal methods on arbitrary-dimensional, polytopal meshes using generic programming. *J. Comput. Appl. Math.*, 2017. published online <http://dx.doi.org/10.1016/j.cam.2017.09.017>.
- [19] B. Cockburn, J. Gopalakrishnan, and R. Lazarov. Unified hybridization of discontinuous Galerkin, mixed, and continuous Galerkin methods for second order elliptic problems. *SIAM J. Numer. Anal.*, 47(2):1319–1365, 2009.
- [20] B. Cockburn, D. A. Di Pietro, and A. Ern. Bridging the Hybrid High-Order and Hybridizable discontinuous Galerkin methods. *ESAIM Math. Model. Numer. Anal.*, 50(3):635–650, 2016.
- [21] D. A. Di Pietro and J. Droniou. A Hybrid High-Order method for Leray-Lions elliptic equations on general meshes. *Math. Comp.*, 86(307):2159–2191, 2017.
- [22] D. A. Di Pietro and A. Ern. *Mathematical aspects of discontinuous Galerkin methods*, volume 69 of *Mathématiques & Applications (Berlin) [Mathematics & Applications]*. Springer, Heidelberg, 2012.
- [23] D. A. Di Pietro and A. Ern. A Hybrid High-Order locking-free method for linear elasticity on general meshes. *Comput. Methods Appl. Mech. Engrg.*, 283:1–21, 2015.
- [24] D. A. Di Pietro and S. Krell. A Hybrid High-Order method for the steady incompressible Navier–Stokes problem. *J. Sci. Comput.*, 2017. published online <https://doi.org/10.1007/s10915-017-0512-x>.
- [25] D. A. Di Pietro, A. Ern, and S. Lemaire. An arbitrary-order and compact-stencil discretization of diffusion on general meshes based on local reconstruction operators. *Comput. Methods Appl. Math.*, 14(4):461–472, 2014.
- [26] D. A. Di Pietro, J. Droniou, and A. Ern. A discontinuous-skeletal method for advection-diffusion-reaction on general meshes. *SIAM J. Numer. Anal.*, 53(5):2135–2157, 2015.
- [27] D. A. Di Pietro, A. Ern, A. Linke, and F. Schieweck. A discontinuous skeletal method for the viscosity-dependent Stokes problem. *Comput. Methods Appl. Mech. Engrg.*, 306:175–195, 2016.
- [28] J. Droniou, R. Eymard, T. Gallouët, and R. Herbin. A unified approach to mimetic finite difference, hybrid finite volume and mixed finite volume methods. *Math. Models Methods Appl. Sci.*, 20(2):265–295, 2010.

- [29] G. Drouet and P. Hild. Optimal convergence for discrete variational inequalities modelling Signorini contact in 2D and 3D without additional assumptions on the unknown contact set. *SIAM J. Numer. Anal.*, 53(3):1488–1507, 2015.
- [30] R. Eymard, T. Gallouët, and R. Herbin. Discretization of heterogeneous and anisotropic diffusion problems on general nonconforming meshes SUSHI: a scheme using stabilization and hybrid interfaces. *IMA J. Numer. Anal.*, 30(4):1009–1043, 2010.
- [31] R. Eymard, G. Henry, R. Herbin, F. Hubert, R. Klöforn, and G. Manzini. 3d benchmark on discretization schemes for anisotropic diffusion problems on general grids. In J. Fořt, J. Fürst, J. Halama, R. Herbin, and F. Hubert, editors, *Finite Volumes for Complex Applications VI Problems & Perspectives*, pages 895–930, Berlin, Heidelberg, 2011. Springer Berlin Heidelberg. ISBN 978-3-642-20671-9.
- [32] R. S. Falk. Error estimates for the approximation of a class of variational inequalities. *Math. Comput.*, 28:963–971, 1974.
- [33] A. Friedman. *Variational principles and free-boundary problems*. Pure and Applied Mathematics. John Wiley & Sons, Inc., New York, 1982. A Wiley-Interscience Publication.
- [34] S. Gaddam and T. Gudi. Bubbles enriched quadratic finite element method for the 3d-elliptic obstacle problem. *Comput. Methods Appl. Math.*, 2017. URL <https://doi.org/10.1515/cmam-2017-0018>.
- [35] R. Glowinski. *Numerical methods for nonlinear variational problems*. Scientific Computation. Springer-Verlag, Berlin, 2008. Reprint of the 1984 original.
- [36] T. Gustafsson, R. Stenberg, and J. Videman. Mixed and stabilized finite element methods for the obstacle problem. *SIAM J. Numer. Anal.*, 55(6):2718–2744, 2017.
- [37] M. Hintermüller, K. Ito, and K. Kunisch. The primal-dual active set strategy as a semismooth Newton method. *SIAM J. Optim.*, 13(3):865–888 (2003), 2002.
- [38] S. Hüeber and B. I. Wohlmuth. An optimal a priori error estimate for nonlinear multibody contact problems. *SIAM J. Numer. Anal.*, 43(1):156–173, 2005.
- [39] D. Kinderlehrer and G. Stampacchia. *An introduction to variational inequalities and their applications*, volume 31 of *Classics in Applied Mathematics*. Society for Industrial and Applied Mathematics (SIAM), Philadelphia, PA, 2000. Reprint of the 1980 original.
- [40] Y. Kuznetsov, K. Lipnikov, and M. Shashkov. The mimetic finite difference method on polygonal meshes for diffusion-type problems. *Comput. Geosci.*, 8(4):301–324 (2005), 2004.
- [41] J. Nitsche. Über ein Variationsprinzip zur Lösung von Dirichlet-Problemen bei Verwendung von Teilräumen, die keinen Randbedingungen unterworfen sind. *Abh. Math. Sem. Univ. Hamburg*, 36:9–15, 1971. Collection of articles dedicated to Lothar Collatz on his sixtieth birthday.
- [42] R. H. Nochetto, K. G. Siebert, and A. Veiser. Pointwise a posteriori error control for elliptic obstacle problems. *Numer. Math.*, 95(1):163–195, 2003.
- [43] J.-F. Rodrigues. *Obstacle problems in mathematical physics*, volume 134 of *North-Holland Mathematics Studies*. North-Holland Publishing Co., Amsterdam, 1987. Notas de Matemática [Mathematical Notes], 114.
- [44] F. Scarpini and M. A. Vivaldi. Error estimates for the approximation of some unilateral problems. *RAIRO Anal. Numér.*, 11(2):197–208, 221, 1977.
- [45] G. Stampacchia. *Equations elliptiques du second ordre à coefficients discontinus*. Les presses de l’Université de Montréal, 1966.
- [46] F. Wang, W. Han, and X.-L. Cheng. Discontinuous Galerkin methods for solving elliptic variational inequalities. *SIAM J. Numer. Anal.*, 48(2):708–733, 2010.

- [47] L.-h. Wang. On the quadratic finite element approximation to the obstacle problem. *Numer. Math.*, 92(4):771–778, 2002.
- [48] L.-h. Wang. On the error estimate of nonconforming finite element approximation to the obstacle problem. *J. Comput. Math.*, 21(4):481–490, 2003.
- [49] B. Wohlmuth. Variationally consistent discretization schemes and numerical algorithms for contact problems. *Acta Numer.*, 20:569–734, 2011.
- [50] B. I. Wohlmuth, A. Popp, M. W. Gee, and W. A. Wall. An abstract framework for a priori estimates for contact problems in 3D with quadratic finite elements. *Comput. Mech.*, 49(6):735–747, 2012.